Magnetic structure map for face-centered tetragonal iron: Appearance of a collinear spin structure

D. Reith[*] and R. Podloucky

Institute of Physical Chemistry, University of Vienna and Center for Computational Materials Science, Sensengasse 8, A-1090 Vienna, Austria

M. Marsman

*Computational Materials Physics, University of Vienna and Center for Computational Materials Science,
Sensengasse 8, A-1090 Vienna, Austria*

P. O. Bedolla-Velazquez and P. Mohn

*Department of Applied Physics, Vienna University of Technology and Center for Computational Materials Science,
Makartvilla, Gußhausstraße 25-25a, A-1040 Vienna, Austria*

For fcc and tetragonal distorted fct iron a large number of magnetic configurations as a function of crystal structural parameters were studied by means of density functional theory concepts. The stability of magnetic structures was defined by the magnetic reorientation energy $\Delta E_{\rm reor}^i$ as the difference of the total energy of configuration i and that of the fcc ferromagnetic state. The cluster expansion technique was applied to six volumes deriving $\Delta E_{\rm reor}$ for more than 90 000 collinear spin structures at each volume. Structures with low $\Delta E_{\rm reor}$ were tetragonally distorted according to a two-dimensional mesh defined by volume per atom V and c/a ratio. At each mesh point $\Delta E_{\rm reor}$ for all collinear structures were compared to results for spin spirals (SSs) which were calculated on a grid of propagation directions, and then the lowest $\Delta E_{\rm reor}$ defined the magnetic structure map. Three local minima were identified and for each of the minima SSs were calculated on a fine grid of propagation vectors. At the minimum with $V = 10.6$ Å^3 and $0.94 \leqslant c/a \leqslant 1.01$ a hitherto unknown simple collinear spin structure with four atoms per fct unit cell was the most stable one. It consists of two atoms with antiferromagnetically ordered local moments of ± 1.8 $\mu_{\rm B}$ and of two atoms with zero local moment.

The intriguing magnetic orderings of fcc-related phases of Fe have received particular attention. Although a large number of experimental as well as theoretical studies have been performed it is still an open question, whether unknown magnetic phases exist.

Experiments were done on thin films [1–15] and precipitates [16–18] with the tetragonally distorted fct structure being enforced by a host material or substrate with fcc structure. Diffraction measurements on precipitates [16,17] observed a helical spin spiral (SS) which stimulated DFT studies [19–26]. Marsman *et al.* [25] found the experimentally claimed SS when the fcc structure was tetragonally distorted. This was confirmed by a recent experiment on precipitates [18]. However, experiments on thin films were inconclusive, suggesting a wide range of magnetic configurations such as ferromagnetic, antiferromagnetic, SS, double-layer antiferromagnetic (with and without noncollinear components), and even nonmagnetic ordering posing an unresolved riddle [1,2,4–6,9,12–15,27]. While a consensus has been more or less established that the upper two layers of the thin-film Fe are ferromagnetically ordered the magnetism in the lower layers remains contested [10,12,13,15].

We search for new structures by means of a map describing magnetic ordering versus volume per atom V and c/a ratio of tetragonally distorted fcc Fe, thereby scanning a large configuration space for magnetic orderings for which we developed a strategy based on spin-dependent total energies as derived by density functional theory (DFT) calculations.

First, a large set of collinear magnetic configurations with fcc lattice was generated and sifted through according to Fig. 1. This was done by cluster expansion [28–31] (CE) at several volumes per atom. Within CE the energy under consideration of a given configuration of spins or atoms is expanded in terms of interacting clusters [28–31]. Their effective interaction energy is derived by fitting to a suitable set of DFT calculations. By that DFT accuracy can be carried over to a very large number of structures (see top panel of Fig. 1). After analysis of the CE results, structures were selected and *tetragonally* distorted according to a two-dimensional mesh defined by V and c/a (see Fig. 3). For each mesh point the magnetic reorientation energies $\Delta E_{\rm reor}$ (see caption of Fig. 1) for selected collinear structures were compared to $\Delta E_{\rm reor}$ for SSs with a selected set of propagations $\vec{q}$ and by that three local minima were found. For each minimum SSs were recalculated on a fine grid of propagations. Finally, the magnetic structure with the lowest $\Delta E_{\rm reor}$ is indicated on the two-dimensional structure map. References [32–34] presented a general multispin-configuration CE, which includes also SSs. Such a general concept, however, is computationally extremely costly. A similar scan, as done in this work, over various c/a ratios and volumes would necessitate a huge number of DFT calculations.

DFT calculations for spin-dependent total energies were done by VASP [35,36] within the projector augmented wave method [37]. The generalized gradient parametrization of Ref. [38] was chosen and the basis set size cutoff was 400 eV. The Brillouin zone integration was made by a Gaussian smearing technique with a broadening of $\sigma = 0.2$ eV extrapolating energies to $\sigma \to 0$ on a $17 \times 17 \times 17$ $\vec{k}$-point

_____

[*]david.reith@univie.ac.at
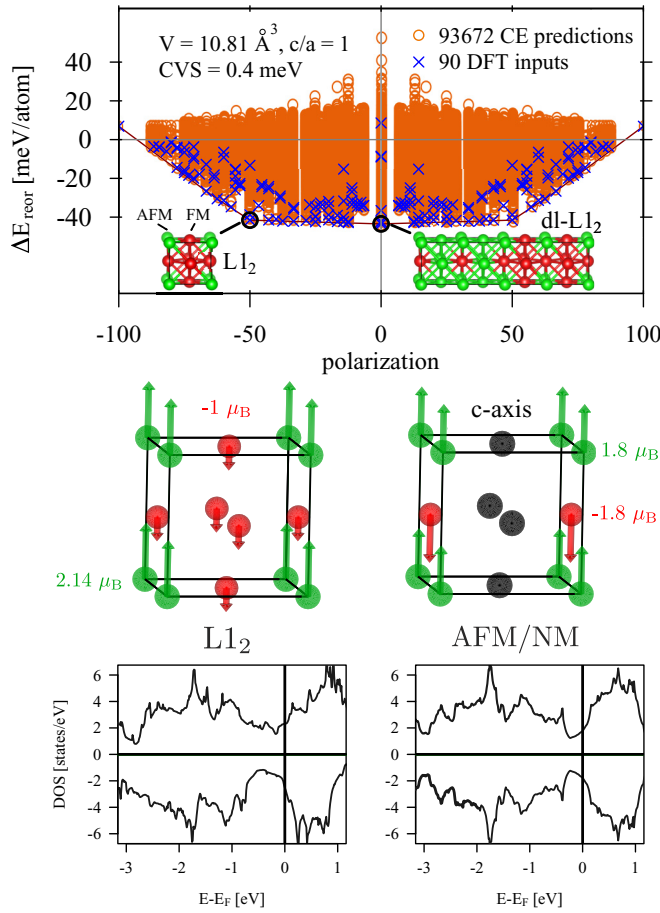
FIG. 1. (Color online) Upper panel: Cluster expansion for collinear magnetic structures on a parent fcc lattice for up to 16 atoms per unit cell for the volume per atom $V = 10.81$ Å^3. Magnetic reorientation energy vs total spin polarization (in percent), $\Delta E_{\text{reor}} = E(V) - E_{\text{FM}}(V_0)$, as defined by the total energies $E(V)$ of each spin configuration with respect to the total energy $E_{\text{FM}}(V_0)$ of fcc ferromagnetic Fe at equilibrium volume $V_0 = 10.52$ Å. Conspicuously, the ground state line is almost horizontal up to $\pm 50\%$ indicating the stability of structures with L1$_2$-like admixtures. Center panel: Collinear L1$_2$-like magnetic configuration (left) with a cubic lattice. It is unstable under tetragonal distortion by which the AFM/NM configuration (right) for $c/a < 1$ is stabilized (see Fig. 2). Black spheres: Atoms with zero local moment. Lowest panel: Spin-polarized total density of states (DOS). Positive/negative values: DOS of majority/minority spin states. The DOS for L1$_2$ is asymmetric because of its antiferrimagnetic ordering, whereas for AFM/NM it is perfectly symmetric.

mesh [39] for a one-atom unit cell. Results were thoroughly cross-checked using the tetrahedron integration method with Blöchl's correction [40]. For larger cells the mesh was scaled down accordingly. SSs were calculated by means of the generalized Bloch theorem [25,41,42]. The local magnetic spin moments were determined for a sphere of radius $R_{\text{loc}} = 1.005$ Å.

The cluster expansion was done with the UNCLE package [31]: a binary cluster expansion [28–31] was performed for collinear up/down spin ordering on an fcc parent lattice at the six volumes per atom, $V = 10.27, 10.81, 11.18, 11.42,$

11.76, 12.01 Å^3, while atomic positions and cell shape were not relaxed. The condition for accepting a given spin configuration for the CE was that the local moments were $\mu \geqslant |0.1| \, \mu_{\text{B}}$. The CE fitting was done by least-squares minimization [43] checking its quality in terms of the (leave one out) cross validation score (CVS) [44]. A genetic algorithm was applied for the selection of clusters up to six-body interactions. Due to spin interchangeability ΔE_{reor} is symmetric with respect to the total spin polarization (see Fig. 1).

Discussing the CE calculations we focus only on $V = 10.81$ Å^3. The total number of DFT input structures was 90 and the configuration search was done for up to 16 atoms per unit cell, resulting in 93 672 magnetic configurations.

The CE-derived ground states strongly depend on volume. At larger volumes $V > 11.1$ Å^3 the most favorable ordering is the double-layer antiferromagnetic (dl-AFM) configuration [22,23,25,26], which is unstable under tetragonal distortion and monoclinic shearing [23,25]. Its stability in comparison to SSs is disputed [24,26]. Remarkably, at the smaller volume of $V = 10.81$ Å^3 a ferrimagnetic configuration resembling the crystallographic L1$_2$ (Cu$_3$Au) structure in combination with a very similar double-layer L1$_2$-like (dl-L1$_2$) is found to be stable. As sketched in Fig. 1 L1$_2$ consists of local magnetic moments of distinctly different sizes: a large moment with $\mu = +2.14 \, \mu_{\text{B}}$ and three small moments with $\mu = -1 \, \mu_{\text{B}}$, resulting in the total moment of $\mu_{\text{tot}} = -0.86 \, \mu_{\text{B}}$ per unit cell.

The moments of dl-AFM ordering and other studied antiferromagnetic (AFM) configurations depend only weakly on the tetragonal distortion. However, for L1$_2$ the small moments in the ferromagnetic plane collapse resulting in a peculiar mixed antiferromagnetic/nonmagnetic (AFM/NM) spin configuration, in which AFM planes with moments of $\mu = 1.8 \, \mu_{\text{B}}$ alternate with NM planes (see Fig. 1). Remarkably, even for $c/a = 1$ and $V < 10.9$ Å^3 the AFM/NM configuration is more stable by one meV/atom than cubic L1$_2$ (see Fig. 2).

Focusing on noncollinear SSs, of interest are spirals with propagations $\vec{q}$ in directions Γ-X/Z, and spirals in directions X/Z-$P/Y/U$. The following propagations were considered: $\vec{q}_{\Gamma X}(\xi) = \frac{2\pi}{a}(\xi, 0, 0 \cdot (c/a)^{-1})$, $\vec{q}_{\Gamma Z}(\xi) = \frac{2\pi}{a}(0, 0, \xi \cdot (c/a)^{-1})$,
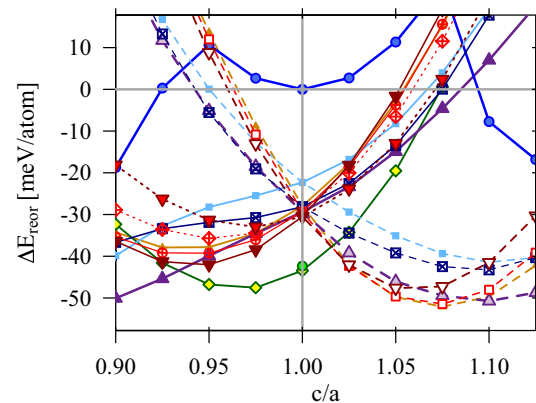
FIG. 2. (Color online) Magnetic reorientation energy ΔE_{reor} as a function of c/a for a variety of collinear configurations and SSs. For each point, i.e., fixed c/a, ΔE_{reor} is minimized with respect to volume V. Symbols refer to magnetic configurations as defined in Fig. 3.
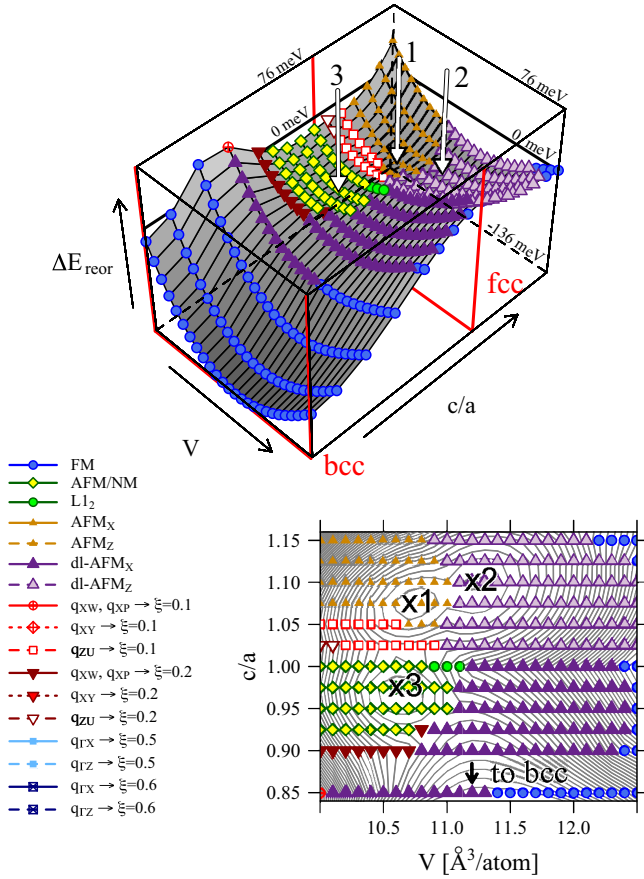
FIG. 3. (Color online) Symbols denote the investigated collinear orderings and SSs (see text). Collinear AFM spin structures with tetragonal distortion applied perpendicular to the sequence of alternating spin up and down FM planes are AFM_X, $dl-AFM_X$; parallel to FM planes: AFM_Z, $dl-AFM_Z$. Upper panel: Three-dimensional magnetic structure map defined by the lowest ΔE_{reor} as a function of c/a and volume V. Lower panel: Two-dimensional representation of upper panel. Contour lines drawn in steps of 2.38 meV/atom. Local minima are denoted by x_1, x_2, and x_3 (see text).

$\vec{q}_{XP}(\xi) = \frac{2\pi}{a}(1,0,\xi \cdot (c/a)^{-1})$, $\vec{q}_{XY}(\xi) = \frac{2\pi}{a}(1,\xi,0 \cdot (c/a)^{-1})$, and $\vec{q}_{ZU}(\xi) = \frac{2\pi}{a}(\xi,0,1 \cdot (c/a)^{-1})$ whereby a defines the lattice parameter and c/a the tetragonal distortion. For $\vec{q}_{\Gamma X}(\xi)$ and $\vec{q}_{\Gamma Z}(\xi)$ the parameter ξ varies between $0 \leqslant \xi \leqslant 1$ and for $\vec{q}_{XP}(\xi)$, $\vec{q}_{XY}(\xi)$, $\vec{q}_{ZU}(\xi)$ its range is $0 \leqslant \xi \leqslant 0.5$. Because of the higher symmetry of the fcc lattice the directions are reduced to $\vec{q}_{\Gamma X}(\xi) = \vec{q}_{\Gamma Z}(\xi)$ and $\vec{q}_{XW}(\xi) = \vec{q}_{XP}(\xi) = \vec{q}_{XY}(\xi) = \vec{q}_{ZU}(\xi)$, accordingly. In previous DFT studies [21–26], SSs with $\xi = 0.5, 0.6$ for directions $\vec{q}_{\Gamma X}(\xi)$, $\vec{q}_{\Gamma Z}(\xi)$, and $\xi = 0.1, 0.2$ for directions $\vec{q}_{XW}(\xi)$ and the related directions $\vec{q}_{XP}(\xi)$, $\vec{q}_{XY}(\xi)$, $\vec{q}_{ZU}(\xi)$ were found to be in contest. At each point of the magnetic structure map the choice of propagations was made as just discussed. At each of the three energy minima of the map (see Fig. 3 and Table 1) a much finer scan of $\vec{q}(\xi)$-vectors in steps of $\Delta\xi = 0.01$ was made. In addition, the accuracy of suitable supercell calculations in comparison to the generalized Bloch theorem was tested and found to be sufficient: the differences of total energies between both approaches were always $\leqslant 0.3$ meV/atom.

TABLE I. Magnetic orderings and corresponding volumes, c/a ratios, and reorientation energies ΔE_{reor}. First three lines: the three local minima (see Fig. 3). Fourth and fifth lines: minima of most stable SSs. Last five lines: minimized ΔE_{reor} for high-moment (HM) and low-moment (LM) ferromagnetic ordering, the non-spin-polarized (NM) calculation, the bcc FM α phase, and the $L1_2$ structure.

	mag. ord.	V (Å^3)	c/a	ΔE_{reor} (meV/atom)
x_1	AFM_Z	10.7	1.075	−52
x_2	dl-AFM_Z	11.2	1.100	−51
x_3	AFM/NM	10.6	0.975	−48
SS1	$\vec{q}_{ZU}(0.1)$	10.7	1.075	−51
SS2	$\vec{q}_{XP}(0.2)$	10.7	0.950	−42
	FM (HM)	11.7	1.175	−25
	FM (LM)	10.5	1.000	0
	NM	10.2	1.000	19
	FM bcc Fe	11.3	$1/\sqrt{2}$	−136
	$L1_2$	10.7	1.000	−42

For all investigated spin structures Fig. 2 depicts ΔE_{reor} depending on c/a. For each point and configuration the energy was minimized with regards to V. The two regions $c/a < 1$ and $c/a > 1$ are clearly distinguishable by the most stable spin structures. For $c/a > 1$ SS configurations $\vec{q}_{\Gamma Z}$, $\vec{q}_{ZU}$ propagating along the c axis and collinear structures AFM_Z are favored. For $0.93 < c/a < 1$ clearly one structure is most stable, namely the newly found AFM/NM ordering (see Fig. 1). At $c/a = 1/\sqrt{2}$ the FM bcc α phase becomes the most stable one (not shown).

Discussing the volume dependency the collinear configurations AFM, AFM/NM, $L1_2$ and the noncollinear SSs $\vec{q}_{XP}(\xi)$, $\vec{q}_{XY}(\xi)$, $\vec{q}_{ZU}(\xi)$ have their respective minima of ΔE_{reor} in the range of $10.4 \leqslant V \leqslant 10.8$ Å^3. For dl-AFM and the SSs $\vec{q}_{\Gamma X}(\xi)$, $\vec{q}_{\Gamma Z}(\xi)$ the minimum of ΔE_{reor} appears at the larger volumes $10.6 \leqslant V \leqslant 11.3$ Å^3. A ferromagnetic low-moment (LM) phase with a moment of $\mu = 0.99 \, \mu_B$ appears at the minimum with $V = 10.5$ Å^3 and $c/a = 1$. For $0.95 < c/a < 1.075$ the LM ferromagnetic configuration is more favorable than the two high-moment (HM) ferromagnetic phases which are (a) an fct phase with $\mu = 2.35 \, \mu_B$ and its minimum at $V = 11.7$ Å^3, $c/a = 1.175$, and (b) the HM bcc α phase with $\mu = 2.16 \, \mu_B$ at $c/a = 1/\sqrt{2}$ and $V = 11.3$ Å^3 (see Table 1).

The centerpiece of our work is shown in Fig. 3, presenting the structure map of magnetic phase stability as a function of volume and c/a ratio. It combines the results for collinear orderings and SSs in terms of the lowest ΔE_{reor}. Three local minima were found (see Table 1) as marked by x_1, x_2, and x_3 (see Fig. 3). The minima x_1 and x_2 occur for $c/a > 1$ whereas x_3 is found for $c/a < 1$. If only SSs are considered the two local minima SS1 and SS2 appear as listed in Table 1. SS1 with $\vec{q}_{ZU}(0.1)$ has its minimum for $c/a > 1$ whereas for SS2 with $\vec{q}_{XP}(0.2)$ the minimum is for $c/a < 1$.

Minimum x_1 with $c/a = 1.075, V = 10.7$ Å^3 represents the collinear AFM_Z configuration. However, Table 1 (lines one and four) shows that the energy difference between AFM_Z and SS1 with $\vec{q}_{ZU}(0.1)$ is only 1 meV. In fact, a

small orthorhombic distortion with $b/a \sim 1.015$ stabilizes SS1 by 0.2 meV/atom as predicted by Marsman *et al.* [25] and confirmed experimentally by Tsunoda *et al.* [18]. For $1 < c/a < 1.075$ SS1 is always more favorable than AFM$_Z$ but for $c/a \geqslant 1.075$ AFM$_Z$ is more favorable than any SS1 with $\vec{q}_{ZU}(\xi)$ and $\xi > 0$, as stated in Ref. [25].

Minimum x_2 with $c/a = 1.10, V = 11.2$ Å^3 belongs to dl-AFM$_Z$. At these coordinates the closest competing configuration is the SS with $\vec{q}_{\Gamma Z}(\xi = 0.6)$ which is less stable by 8 meV/atom. This result was confirmed by calculating SSs for $0 < \xi < 1$. For dl-AFM$_Z$ no atomic relaxation was considered, which would further lower ΔE_{reor}. Therefore, in contrast to Refs. [24,26] we exclude that any $\vec{q}_{\Gamma Z}$ SS will be more stable than dl-AFM$_Z$ at volumes larger than 11 Å^3. The collinear configurations dl-AFM$_X$ and dl-AFM$_Z$ are the dominating structures but they are unstable against monoclinic shearing [23,25].

Minimum x_3 corresponding to the AFM/NM configuration with its peculiar mixture of AFM and NM planes (see Fig. 1) is the shallowest one (see Table 1). Nevertheless, it is the only configuration with a local minimum for $c/a < 1$, namely $c/a = 0.975, V = 10.6$ Å^3. Supposedly, the AFM/NM configuration indicates formation of an SS. However, the corresponding SSs with propagations $\vec{q}_{\Gamma X}(0.5)$ and $\vec{q}_{\Gamma Z}(0.5)$ are very unfavorable for this particular c/a (see Fig. 2): AFM/NM is by 9 meV/atom more stable than the closest noncollinear ordering SS2 with $\vec{q}_{XP}(\xi = 0.2)$. Varying ξ at the same c/a and V shows that indeed SS2 with $\xi = 0.2$ is the most favorable SS.

The stability of AFM/NM compared to L1$_2$ is illustrated by the density of states (DOS) (see Fig. 1): the values of the DOS at Fermi energy, $N(E_F)$, for both spin channels of L1$_2$ is larger by 40% than for AFM/NM (see also Supplementary Material B [46]). For L1$_2$ the spin up and down DOS is not symmetric and the total moment is not zero. This is in contrast to AFM/NM for which the total moment is zero because for each layer perpendicular to the c axis the local moments $\pm 1.8 \mu_B$ either cancel or are perfectly zero. Performing studies with different spin splits (see Supplementary Material B [46]) it turns out that the stability of AFM/NM is due to its lowest $N(E_F)$. The structure is unstable towards an orthorhombic distortion. When b/a deviates from 1 symmetry is reduced and the magnetically dead atoms accumulate finite local moments. Its crystal structure then resembles the structure at minimum x_1 (see Supplementary Material A [46]).

The peculiarity of AFM/NM is illustrated by Fig. 4 showing that the magnetization density around the positions of the magnetically dead atoms is strongly spin polarized in a symmetric manner such that the resulting local moments are zero. This symmetry property remains even when the AFM/NM structure is tetragonally distorted according to Fig. 1. Consequently, AFM/NM is the most stable spin ordering for $0.94 \leqslant c/a \leqslant 1.01$.

By means of a thorough search for magnetic orderings at various volumes and c/a ratios we have constructed a magnetic structure map for bulk phases of fct Fe. Notably, our results (see Figs. 2) show that the c/a ratio profoundly affects magnetism with $c/a > 1$ favoring magnetic configurations propagating along the c-axis while for $c/a < 1$ propagation occurs orthogonal to the c axis.
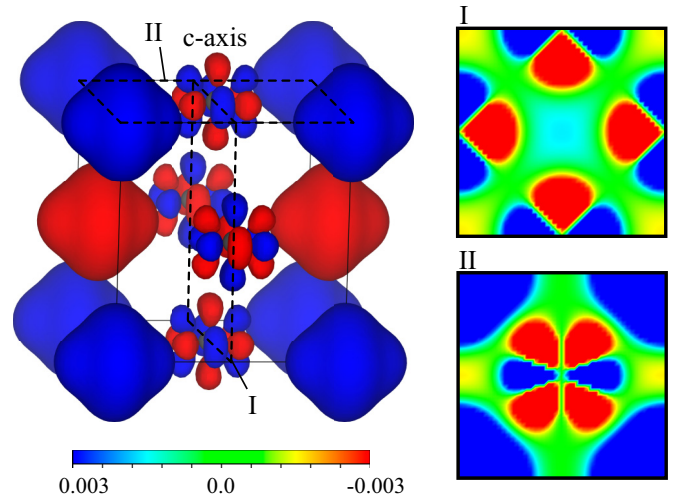
FIG. 4. (Color online) Magnetization density $\rho_{\text{mag}} = \rho_{\text{up}} - \rho_{\text{down}}$ ($\rho_{\text{up}}, \rho_{\text{down}}$: spin up and down charge densities) of AFM/NM ordering. Left panel: Three-dimensional mantle; right panel: contour plots in planes as sketched in left panel. Figure created by VESTA [45].

In general, we cannot exclude the occurrence of more complex noncollinear magnetic configurations in particular for thin films, for which the structural properties differ significantly from a bulklike environment. Thin films consisting of less than 10 ML are currently considered to have a pure face-centered cubic structure [10,11]. However, in view of our results for bulk structures (see Figs. 2 and 3), where the magnetic reorientation energy of the most favorable magnetic configurations are at a local maximum for $c/a = 1$, we find this unlikely. Actually, slight tetragonal distortions have been observed previously [10,11] but have been simplified as face-centered cubic. Reference [11] claims for thin films with 2–4 ML a c/a ratio of ~ 1.015 that decreases with increasing thickness to ~ 0.99 for 10 ML. In light of our findings concerning the sensitivity of magnetism to the c/a ratio, we believe that such small structural differences have a profound influence on magnetic ordering. A recent work indicates that the interlayer distances for 6–7 ML thin films are not constant [12] further complicating the situation.

Summarizing, magnetic configurations are very sensitive to the optimized structural parameters. Therefore, we applied the PBE/GGA approximation, because it is well known [47] to reliably provide the ground state properties of bulk Fe. Our extensive search for magnetic configurations for bulk structures of fct Fe in terms of a magnetic structure map predicts a range of magnetic orderings depending on volume and c/a ratio. This study resulted in the finding of a peculiar collinear magnetic configuration consisting of layers of antiferromagnetically ordered local moments and magnetically dead layers which has eluded all previous investigations on this rather well studied system.

[1] W. Keune, R. Halbauer, U. Gonser, J. Lauer, and D. L. Williamson, J. Appl. Phys. **48**, 2976 (1977).

[2] D. Pescia, M. Stampanoni, G. L. Bona, A. Vaterlaus, R. F. Willis, and F. Meier, Phys. Rev. Lett. **58**, 2126 (1987).

[3] Y. Darici, J. Marcano, H. Min, and P. A. Montano, Surf. Sci. **182**, 477 (1987).

[4] C. Liu, E. R. Moog, and S. D. Bader, Phys. Rev. Lett. **60**, 2422 (1988).

[5] W. A. A. Macedo and W. Keune, Phys. Rev. Lett. **61**, 475 (1988).

[6] M. Stampanoni, Appl. Phys. A **49**, 449 (1989).

[7] S. H. Lu, J. Quinn, D. Tian, F. Jona, and P. M. Marcus, Surf. Sci. **209**, 364 (1989).

[8] H. Landskron, G. Schmidt, K. Heinz, K. Müller, C. Stuhlmann, U. Beckers, M. Wutting, and H. Ibach, Surf. Sci. **256**, 115 (1991).

[9] M. Wutting and J. Thomassen, Surf. Sci. **282**, 237 (1993).

[10] S. Müller, P. Bayer, A. Kinne, P. Schmailzl, and K. Heinz, Surf. Sci. **322**, 21 (1995).

[11] H. Jenniches, J. Shen, C. V. Mohan, S. S. Manoharan, J. Barthel, P. Ohresser, M. Klaua, and J. Kirschner, Phys. Rev. B **59**, 1196 (1999).

[12] H. L. Meyerheim, R. Popescu, D. Sander, J. Kirschner, O. Robach, and S. Ferrer, Phys. Rev. B **71**, 035409 (2005).

[13] H. L. Meyerheim, J.-M. Tonnerre, L. Sandratskii, H. C. N. Tolentino, M. Przybylski, Y. Gabi, F. Yildiz, X. L. Fu, E. Bontempi, S. Grenier *et al.*, Phys. Rev. Lett. **103**, 267202 (2009).

[14] J. Miyawaki, A. Chainani, Y. Takata, M. Mulazzi, M. Oura, Y. Senba, H. Ohashi, and S. Shin, Phys. Rev. Lett. **104**, 066407 (2010).

[15] C. E. ViolBarbosa, H. L. Meyerheim, E. Jal, J.-M. Tonnerre, M. Przybylski, L. M. Sandratskii, F. Yildiz, U. Staub, and J. Kirschner, Phys. Rev. B **85**, 184414 (2012).

[16] Y. Tsunoda, J. Phys.: Condens. Matter **1**, 10427 (1989).

[17] Y. Tsunoda, Y. Nishioka, and R. M. Nicklow, J. Magn. Magn. Mater. **128**, 133 (1993).

[18] Y. Tsunoda, H. Nogami, and M. Takasaka, Phys. Rev. B **76**, 054419 (2007).

[19] O. N. Mryasov, V. A. Gubanov, and A. I. Liechtenstein, Phys. Rev. B **45**, 12330 (1992).

[20] O. N. Mryasov, A. I. Liechtenstein, L. M. Sandratskii, and V. A. Gubanov, J. Phys.: Condens. Matter **3**, 7683 (1991).

[21] K. Knöpfle, L. M. Sandratskii, and J. Kübler, Phys. Rev. B **62**, 5564 (2000).

[22] D. Spišák and J. Hafner, Phys. Rev. B **61**, 16129 (2000).

[23] D. Spišák and J. Hafner, Phys. Rev. Lett. **88**, 056101 (2002).

[24] E. Sjöstedt and L. Nordström, Phys. Rev. B **66**, 014447 (2002).

[25] M. Marsman and J. Hafner, Phys. Rev. B **66**, 224409 (2002).

[26] I. A. Abrikosov, A. E. Kissavos, F. Liot, B. Alling, S. I. Simak, O. Peil, and A. V. Ruban, Phys. Rev. B **76**, 014434 (2007).

[27] L. M. Sandratskii, Phys. Rev. B **81**, 064417 (2010).

[28] J. Sanchez, F. Ducastelle, and D. Gratias, Physcia A **128**, 334 (1984).

[29] L. G. Ferreira, S.-H. Wei, and A. Zunger, Phys. Rev. B **40**, 3197 (1989).

[30] S. Müller, J. Phys.: Condens. Matter **15**, R1429 (2003).

[31] D. Lerch, O. Wieckhorst, G. Hart, R. Forcade, and S. Müller, Modelling Simul. Mater. Sci. Eng. **17**, 055003 (2009).

[32] R. Singer, F. Dietermann, and M. Fähnle, Phys. Rev. Lett. **107**, 017204 (2011).

[33] F. Dietermann, L. Sandratskii, and M. Fähnle, J. Magn. Magn. Mater. **324**, 2693 (2012).

[34] M. Fähnle and S. Zhang, J. Magn. Magn. Mater. **326**, 232 (2013).

[35] G. Kresse and J. Furthmüller, Phys. Rev. B **54**, 11169 (1996).

[36] G. Kresse and D. Joubert, Phys. Rev. B **59**, 1758 (1999).

[37] P. E. Blöchl, Phys. Rev. B **50**, 17953 (1994).

[38] J. P. Perdew, K. Burke, and M. Ernzerhof, Phys. Rev. Lett. **77**, 3865 (1996).

[39] H. Monkhorst and J. Pack, Phys. Rev. B **13**, 5188 (1976).

[40] P. E. Blöchl, O. Jepsen, and O. K. Andersen, Phys. Rev. B **49**, 16223 (1994).

[41] J. Kübler, *Theory of Itinerant Electron Magnetism* (Oxford University Press, Oxford, 2000).

[42] D. Hobbs, G. Kresse, and J. Hafner, Phys. Rev. B **62**, 11556 (2000).

[43] Z. W. Lu, S.-H. Wei, A. Zunger, S. Frota-Pessoa, and L. G. Ferreira, Phys. Rev. B **44**, 512 (1991).

[44] A. van de Walle and G. Ceder, J. Phase Equilib. **23**, 348 (2002).

[45] K. Momma and F. Izumi, J. Appl. Crystallogr. **44**, 1272 (2011).

[46] See Supplemental Material at http://link.aps.org/supplemental/10.1103/PhysRevB.90.014432 for a discussion of the AFM/NM magnetic configuration structural stability (Supplemental Material A) and electronic stability (Supplemental Material B).

[47] D. J. Singh, W. E. Pickett, and H. Krakauer, Phys. Rev. B **43**, 11628 (1991).